OPTOELECTRONICS AND ADVANCED MATERIALS – RAPID COMMUNICATIONS Vol. 4, No. 10, October 2010, p. 1612 - 1616

Structural and optical properties of $Zn_xMn_{1-x}Se$ ($0 \leq x \leq 0.20$) films

T. MOHAN BABU[a], B. K. REDDY[a,*], N. MADHUSUDHANA RAO[b], R. P. VIJAYALAKSHMI[a], D. RAJA REDDY[a], S. UTHANNA[a]

[a] *Department of Physics, Sri Venkateswara University, Tirupati 517 502, India*

[b] *School of Science and Humanities,VIT University,Tamilnadu 632 014, India*

$Zn_{1-x}Mn_xSe$ Diluted magnetic semiconducting films with x = 0.00, 0.10, 0.15 and 0.20 were formed at 523 K on glass substrates by co-evaporation. X-ray diffraction studies revealed that the films were polycrystalline in nature with zinc blende structure with preferential orientation along (111). Optical transmittance studies indicated a nonlinear variation of band gap with 'x' exhibiting a downward bowing at lower concentrations. All the films showed photoluminescence with composition dependent intensities and emission wavelengths.

(Received June 16, 2010; accepted October 14, 2010)

Keywords: Diluted magnetic semiconductors, $Zn_{1-x}Mn_xSe$ thin films structural, Optical properties, Photoluminescence

1. Introduction

Diluted magnetic semiconductors have attracted a great deal of attention due to their unique electronic and magnetic properties [1]. DMS are formed by randomly replacing a fraction of the cations in a compound semiconductor with magnetic ions. In particular, the sp-d interaction between the magnetic ions and the band electrons leads to many interesting physical effects such as extremely large Faraday rotation, giant negative magnetoresistance. The fact that their electronic properties are tunable both by composition and magnetic field has made DMS materials as potential candidates for use in novel optoelectronic devices.

ZnSe based semiconducting materials find wide range of applications in optoelectronic devices such as photodetectors, light sources for the UV and visible spectral regions and electrooptical waveguide modulators [2]. Among ZnSe based DMS, ZnMnSe is extensively studied due to high solubility of Mn in ZnSe. Incorporation of Mn into ZnSe lattice gives rise to required changes in the electronic and optical properties. A nonlinear dependence of optical band gap in Mn content has been reported in $Zn_{1-x}Mn_xSe$ films formed by sophisticated techniques like molecular beam epitaxy, hot wall epitaxy, metal-organic vapour phase epitaxy and RF sputtering etc. [1, 3-6]. In this paper we have reported the preparation of $Zn_{1-x}Mn_xSe$ films formed by co-evaporation technique and studied the influence Mn concentration in the structural and optical properties of ZnMnSe films.

2. Experimental

In the present investigation, $Zn_{1-x}Mn_xSe$ films have been prepared using a relatively simple, low cost thermal co-evaporation technique. Thin films of $Zn_{1-x}Mn_xSe$ were formed on glass substrates by using a Hind Hivac (India) vacuum coating unit model 12 A4D. Two independent evaporation sources of Mo boats were used for ZnSe and MnSe for deposition of $Zn_{1-x}Mn_xSe$ films. 4 N pure ZnSe was used as host, to obtain Mn doped ZnSe films, freshly prepared MnSe in cubic phase was used in appropriate proportion for $Zn_{1-x}Mn_xSe$ films of different compositions. Blue star glass slides were used as substrates. Different substrate temperatures were tried in the range 300 – 573 K. The optimum growth temperature to yield good uniform films was established after a great deal of trial and error procedure. Lower deposition temperatures resulted in poor adhesion and Se rich films, higher temperatures resulted in Se low and re-evaporation of the films. A substrate temperature of 523 K was found to be optimum to form uniform films. The $Zn_{1-x}Mn_xSe$ films with x = 0.00, 0.10, 0.15 and 0.20 were deposited by co-evaporation of ZnSe and Mn from the pre calibrated deposition rates using quartz crystal thickness monitor. All the $Zn_{1-x}Mn_xSe$ films grown in the present study were uniform and pin hole-free.

In the present investigation, Siemens X-ray diffractometer (Model D-5000) with Cu K_α source (λ = 1.54056 Å) was used for structural studies. The transmittance spectra were recorded at room temperature in the wavelength range 300 - 1500 nm using Hitachi U: 3400 UV-Vis-NIR double beam spectrophotometer in order to determine the optical parameters such as optical absorption coefficient and optical band gap. Photoluminescence spectra (PL) of films were recorded at room temperature using Hitachi 650 - Ios UV fluorescence spectrophotometer with two double grating monochromators and a 450W Xenon lamp as source. The emission was detected by a Hamamatsu 928F photomultiplier tube. A Carl Zeiss (Model MA15) energy-dispersive X-ray spectroscopy (EDS) was used for composition analysis studies. An SPA 400 atomic force microscope (AFM) was used for surface morphological studies of the films.

3. Results and discussion

The Mn content in the films estimated by EDS analysis was found to be within ± 3% of the above specified compositions. EDS spectra of the $Zn_{1-x}Mn_xSe$ films deposited at 523 K for x = 0.10 and 0.20 are shown in Fig. 1.

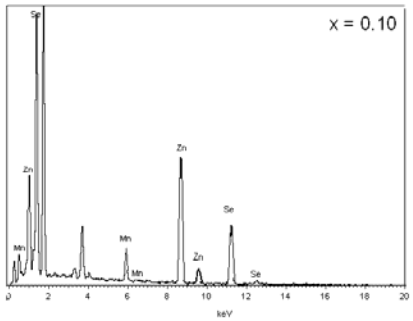

(a)

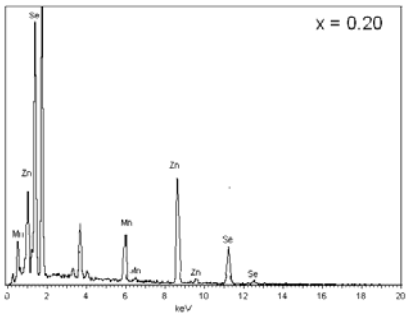

(b)

Fig. 1. EDS spectra of $Zn_{1-x}Mn_xSe$ films for (a) x = 0.10 and, (b) x=0.20.

3.1 Structural analysis

To study the crystallinity and orientations of the $Zn_{1-x}Mn_xSe$ films, XRD studies have been carried out on films of all compositions (x = 0.00, 0.10, 0.15 and 0.20) deposited at 523 K and the XRD patterns are shown in Fig. 2. All the deposited films are polycrystalline with zincblende structure. The films show a marked tendency to preferential (111) orientation, which is also the close packing direction of the zincblende structure. Only Wang et al. [7] reported (111) orientation with zincblende structure at lower Mn concentration ($0 \leq x \leq 0.19$, mixed phases of zincblende and wurtzite structures at higher concentrations ($0.19 \leq x \leq 0.52$). In bulk form Shilaja Mahamuni et al. [8] and Sayan Battacharya et al. [9] also reported the (111) orientation along with (220) and (311) reflection. Hetterich et al [10], Kim et al. [11] and Yu et al. [12] reported (200) and (400) as preferred orientations of zincblende in $Zn_{1-x}Mn_xSe$ films.

It is also observed from the XRD pattern that with increasing Mn content, the (111) peak position shifted to lower values of 2θ. It implies that the lattice parameter increases with increasing Mn content. This is consistent with the ionic / covalent radii of their constituents. The covalent radii of Zn and Mn are 1.266 A^0 and 1.326 A^0 respectively [1].

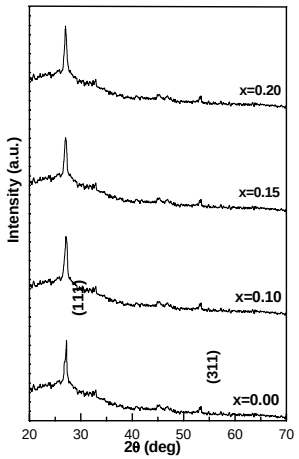

Fig. 2. XRD patterns of all $Zn_{1-x}Mn_xSe$ films.

Hence substitution of Mn for Zn should increase the lattice parameter, accordingly all 2θ values decrease with increase in Mn content [Fig. 2]. The plot of lattice parameter with 'x' is shown in Fig. 3. It is obvious that the lattice parameter increases linearly with Mn concentration following Vegard's law. [1], conformity that Mn substitutes for Zn in the present films. This also implies that the lattice parameter is tailorable with composition in this system. A similar behavior was observed by Hetterich et al. and [10] Yu et al. [12] in $Zn_{1-x}Mn_xSe$ films. From the full width at half maximum (FWHM) intensity of the (111) peak, the average grain sizes were estimated and were in the range of 22 – 55 nm in films of all compositions. The average grain size of the films decreased with increase in Mn concentrations.

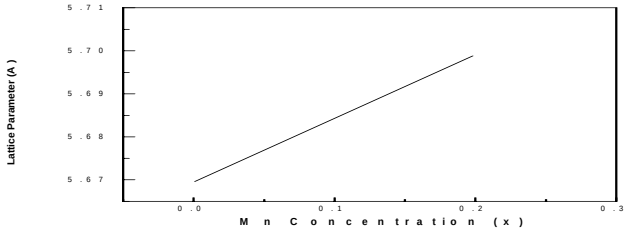

Fig. 3. Variation of lattice parameter with Mn concentration in $Zn_{1-x}Mn_xSe$ films.

3.2 Surface morphological studies

The surface morphological studies of the $Zn_{1-x}Mn_xSe$ films were carried out by using atomic force microscope. AFM images of the $Zn_{1-x}Mn_xSe$ films deposited at 523 K for x = 0.00 and 0.20 are shown in Fig. 4. The morphology of the films significantly varied with Mn concentration. The rectangular grains were observed in x = 0.00 and needle like grains observed in x = 0.20 films. From the figure the estimated grain sizes of the films were decreased with Mn concentration. The grain size of the films for x = 0.00 and 0.20 are 58 nm and 25 nm respectively. These values are good agreement with XRD reported values. The estimated root mean square surface roughness of the films is also observed to be increased as a function of Mn concentration and found to be increased from 6 nm to 14 nm.

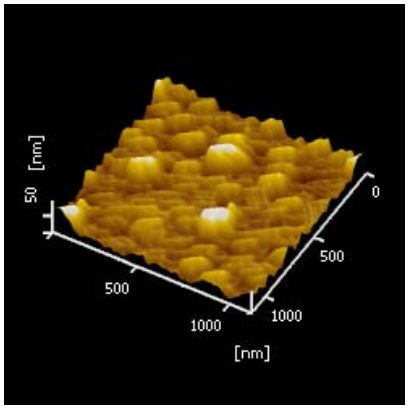

a

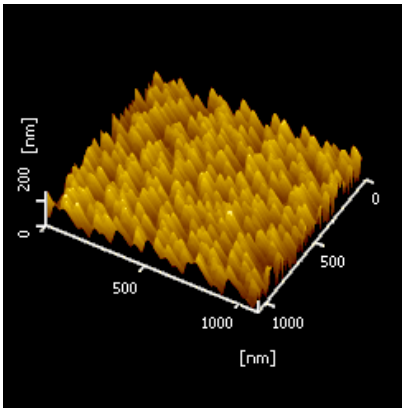

b

Fig. 4. The AFM picture of $Zn_{1-x}Mn_xSe$ films grown at various Mn concentrations x = 0.00 and (b) x = 0.20.

3.3 Optical studies

3.3.1 Transmission spectra

The optical transmission spectra of $Zn_{1-x}Mn_xSe$ films recorded at room temperature (300 K) are shown in Fig. 5. The optical transmission spectra show a sharp fall in the transmittance near the fundamental absorption region. It is evident that the optical transmittance of the films decreases with increasing Mn content. The thickness of the $Zn_{1-x}Mn_xSe$ films as estimated from the optical transmittance spectra was in the range 350 – 380 nm.

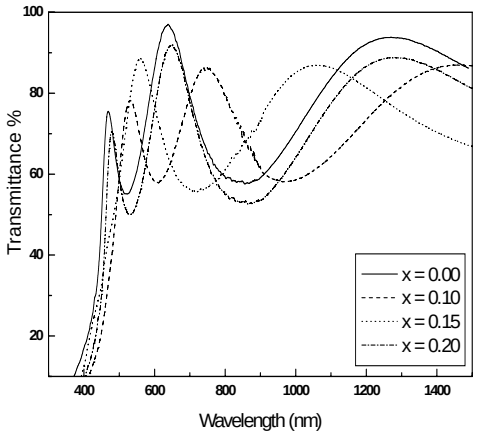

Fig. 5. Optical transmittance spectra of $Zn_{1-x}Mn_xSe$ films.

The absorption coefficient (α) was obtained from the optical transmission spectra near strong absorption region. The plots of $(\alpha h\upsilon)^2$ versus hυ for $Zn_{1-x}Mn_xSe$ films of different composition (x=0.00, 0.10, 0.15 and 0.20) are shown in Fig. 6. Extrapolation of the linear portion of the curve to α = 0 gives the optical band gap of the $Zn_{1-x}Mn_xSe$ films. A plot of optical band gap (E_g) versus Mn concentration (x) is shown in Fig. 7. It is obvious from the figure that the energy gap values do not vary linearly with 'x' and show downward bowing at lower Mn content. The reason for this anomalous behavior is the strong Sp-d interaction between the magnetic ions and the band electrons in $Zn_{1-x}Mn_xSe$ films [13]. A similar trend has been observed in $Zn_{1-x}Mn_xSe$ films deposited by various techniques [14-18].

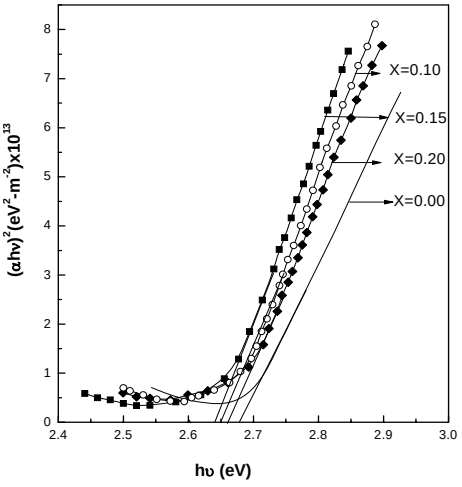

Fig. 6. Plots of $(\alpha h\nu)^2$ versus $(h\nu)$ of $Zn_{1-x}Mn_xSe$ films.

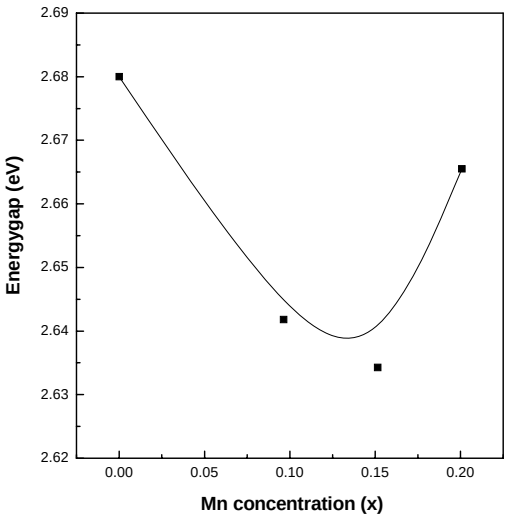

Fig. 7. Variation of optical band gap with the Mn concentration in $Zn_{1-x}Mn_xSe$ films.

3.3.2 Photoluminescence studies

Photoluminescence (PL) spectra of all the films of $Zn_{1-x}Mn_xSe$ (x = 0.00, 0.10, 0.15 and 0.20) were recorded at room temperature in the wavelength range 400 – 600 nm with an excitation wavelength of 360 nm, and are shown in Fig. 8. These show the presence of emission bands spread over the wavelength range 550 – 563 nm with unambiguous peaks lying in the wavelength range 558 – 563 nm. Further, the peak position varied with concentration of Mn. Initially the peak shifted towards higher wavelength but for higher concentrations the peak shifted towards lower wavelengths. This transition seems to occur around $x \geq 0.15$.

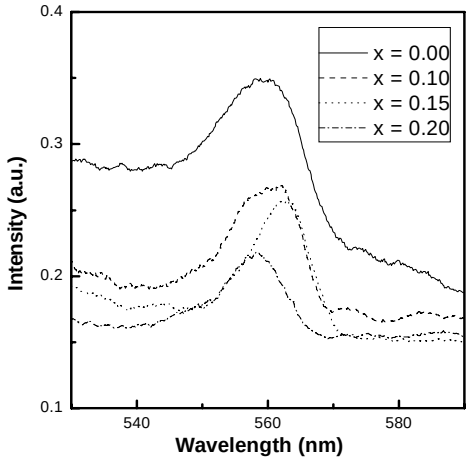

Fig. 8. PL emission spectra of $Zn_{1-x}Mn_xSe$ films.

Luminescence in semiconductors occurs due to defects and band edge recombinations. The defects in the present case are Mn^{2+} atoms themselves and the bands are formed due to ligand field. Generally $^4T_1 \rightarrow {}^6A_1$ transition is observed in this and similar other II-VI diluted magnetic semiconductors. However, this transition occur around 2.2 eV in all the II-VI magnetic semiconductors [1]. Another source of luminescence is the band gap luminescence itself. The position of the PL peak gets modified towards higher wavelength due to stable exciton formation. Excitons are stable electron – hole pairs forming hydrogen atoms like structures and states with or with out mobility. In II-VI diluted magnetic semiconductors these pairs recombine to emit a higher wavelength than the interband transition. As seen from Fig. 8 this particular exciton emission wavelength first increased with Mn concentration and then decreased for higher Mn concentration. This is consistent with the general variation of band gap with composition observed in optical transmittance spectra (Fig. 6). The excitonic peak energy showed bowing with a minimum occurring around $x \sim 0.15$. A similar behavior was reported by, Yu et al. [12], Kolodziejski et al. [17] and Chou et al. [18] in $Zn_{1-x}Mn_xSe$ films. In bulk some of the others [8, 19] have reported Mn^{2+} related emission at ~ 560 nm.

4. Conclusions

The $Zn_{1-x}Mn_xSe$ films with different compositions (x = 0.00, 0.10, 0.15 and 0.20) were grown by thermal co-evaporation on glass substrates at 523 K. XRD studies showed that the films were polycrystalline with zincblende structure with a preferred (111) orientation. The lattice parameter (5.671 Å-5.699 Å) increased linearly with Mn content following Vegard's law. The AFM studies indicated that the grains sizes are decreased and root mean square values are increased with Mn content. Optical Transmission spectra showed sharp fall in transmittance near the fundamental absorption region. The variation of optical band gap with the Mn concentration exhibited downward bowing at low Mn content, which is attributed to strong sp-d interaction. PL emission spectra peak position initially increased to higher wavelength with increase of Mn. Further increase in Mn content, shifted the peak position to lower wavelengths. This observation is in conformity with band gap dependence on composition. Thus, it is concluded that the photoluminescence in the present investigation may be due to exciton recombination. Studies over a wide range of dopant concentration are under process.

Acknowledgement

The authors are grateful to the University Grants Commission, New Delhi, Government of India for providing financial assistance.

References

[1] J. K. Furdyna, J. Appl Phys. **64**, R29 (1988).
[2] H. Babucke, P. Thiele, T. Prasse, M. Rabe, F. Henneberger, Semicond. Sci. Technol. **13**, 200 (1998).

[3] D. Litvinov D. Gerthsen, B. Daniel, C. Klingshirn, M. Hetterich J. Appl, Phys **100,** 23523 (2006).
[4] A. Twardowski, T. Dietl, M. Demianiuk, Solid State Commun. **48**, 845 (1983).
[5] K. J. Ma, W. Giriat, Solid State Commun. **60**, 927 (1986).
[6] J. Stankiewicz, J. R. Fermin, J. Appl, Phys. **63**, 3300 (1988).
[7] J. Wang, C. S. Zhu, A. U. H. Qureshi, D. M. Huang, X. Wang, X. L. Shen, J. Cryst. Growth. **152**, 286 (1995).
[8] Shailaja Mahamuni, Amit D. Lad, Shashikant Patole, J. Phys. Chem. C **112**, 2271 (2008).
[9] Sayan Bhattacharyya, Ilana Perelshtein, Ofer Moshe, Daniel H. Rich, Aharon Gedanken, Adv. Funct. Mater. **18**, 1641 (2008).
[10] M. Hetterich, B. Daniel, C. Klingshirn, P. Pfundstein, D. Litvinov, D. Gerthsen, K. Eichhorn, D. Spemann, Phys. Stat. Sol. C **1**, 649 (2004).
[11] D. J. Kim, Y. M. Yu, S. H. Eom, T. H. Kim, C. S. Go, Y. D. Choi, Mater. Chem. Phys. **92**, 274 (2005).
[12] Y. M. Yu, D. J. Kim, K. J. Lee, Y. D. Choi, O. Byungsung, K. S. Lee, I. H. Choi, M. Y. Yoon, J. Vac. Sci. Technol. A **22**, 1908 (2004).
[13] D. A. Tulchinsky, J. J. Baumherg, D. D. Awschalom, N. Samarth, H. Luo, J. K. Furdyna, Phys. Rev. B **50**, 10851 (1994).
[14] W. K. Hung, M. Y. Chern, Y. F. Chen, W. C. Chou, C. S. Yang, C. C. Cheng, J. L Shen, Solid State Commun. **120**, 311 (2001).
[15] X. Wang, X. Chen, J. Liu, C, Chen, J. Wang, Z. Ling, X. Wang, S. Wang, S. Lu, Solid Stat Commun. **95**, 525 (1995).
[16] L. Martinez, L. R. Gonzalez, W. Giriat, Phys. Stat. Sol. B **180**, 267 (1993).
[17] L. A. Kolodziejski, R. L. Gunshor, R. Venkatasubramanian, T. C. Bonsett, R. Frohne, S. Datta, N. Otsuka, R. B. Bylsma, W. M. Becker, A. V. Nurmikko, Vac. Sci. Technol. B **4**, 583 (1986).
[18] W. C. Chou, C. S. Ro, D. Y. Hong, C. S. Yang, C. Y. Lin, T. Y. Lin, K. C. Chiu, T. R. Yang, C. M. Lin, D. S. Chuu, W. Y. Uen, Chinese J. Phys. **36**, 120 (1998).
[19] J. F. Suyver, S. F. Wuister, J. J. Kelly, A. Meijerink, Phys. Chem. Chem. Phys. **2**, 5445 (2000).

*Corresponding author: borrak2001@yahoo.com